Chapter 6

One–particle transfer

and refs. therein   *cf.*

(Chapters 7 and 8 (7: formalism two-nucleon transfer, 8: applications and examples))

In what follows we present a derivation of the one–particle transfer differential cross section within the framework of the DWBA (Satchler, 1980; Broglia and Winther, 2004). The structure input for the calculations are mean field potentials and single–particle states dressed through the coupling with the variety of collective, (quasi) bosonic vibrations, leading to modified formfactors[1] resulting from the interweaving of these vibrations and a number of orbitals with the original, unperturbed single–particle state (Bohr and Mottelson, 1975; Bès and Broglia, 1977). With the help of these modified formfactors, and of optical potentials, one can calculate the absolute differential cross sections, quantities which can be directly compared with the experimental findings.

In this way one avoids to introduce, let alone use spectroscopic factors, quantities which are rather elusive to define. This is in keeping with the fact that as a nucleon moves through the nucleus it feels the presence of the other nucleons whose configurations change as time proceeds. It takes time for this information to be fed back on the nucleon. This renders the average potential nonlocal in time (cf. C. Mahaux et al. (1985) and references therein). A time–dependent operator can always be transformed into an energy dependent operator, implying an ω–dependence of the properties which are usually adscribed to particles like (effective) mass, charge, etc. Furthermore, due to the Pauli principle, the average potential is also non local in space (cf. App.(?)). Consequently, one is forced to deal with nucleons which carry around a cloud of (quasi) bosons, aside from exchanging its position with that of the other nucleons. It is of notice that the above mentioned phenomena are not only found within the realm of nuclear physics, but are common within the framework of many–body systems as well as of field theories like quantum electrodynamic (QED). In fact, a basic result of such theories is that nothing is free (Feynman, 1975). A textbook example being provided by the Lamb shift, resulting from the dressing of the hydrogen atom electron, as a result of the exchange of this electron with those participating in the spontaneous, virtual excitation (zero point fluctuations (ZPF)) of the QED vacuum (cf. App.(?)). Within this context see Sect. (?) (Examples and Applications) concerning the phenomenon of parity inversion in N=6 (closed shell) exotic halo nuclei.

(cf. Apps. A and B)

(cf. Apps. C and D)

really

6.2

the   *(of)*   *transfer*   *renormalized*   *cf. e.g.*

---

[1] It is of notice that single–particle modified formfactors have their counterpart in the transition densities (?) and in the modified two–nucleon formfactors (?) associated with inelastic and pair transfer (Broglia et al., 1973), respectively

reactions)   *with*

((Ch. 5 (inelastic scattering)))

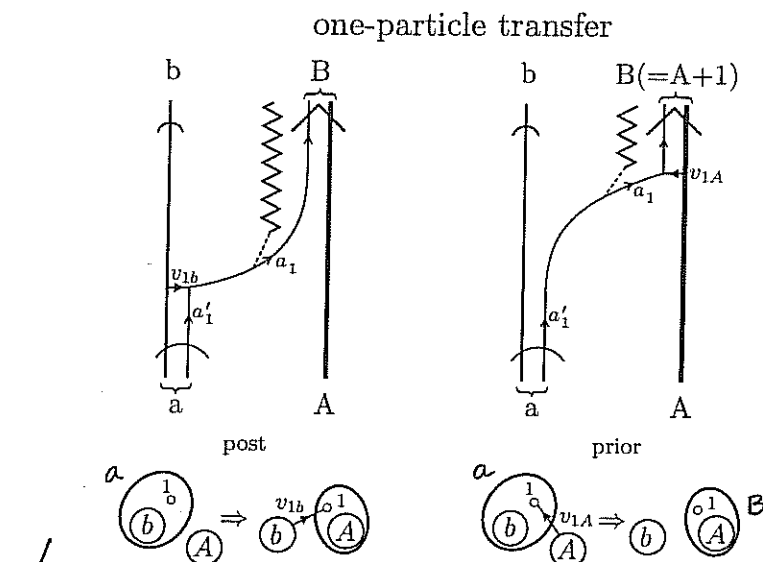1

one-particle transfer

Figure 6.1.1: One–particle reaction $a(= b + 1) + A \rightarrow b + B(= A + 1)$. The time arrow is assumed to point upwards. The quantum numbers characterizing the states in which the transferred nucleon moves in projectile and target are denoted a_1' and a_1 respectively. The interaction inducing the nucleon to be transferred can act either in the entrance channel $((a, A); v_{1A}$, prior representation) or in the exit channel $((b, B); v_{1b}$, post representation), in keeping with energy conservation. In the transfer process, the nucleon changes orbital at the same time that a change in the mass partition takes place. The corresponding relative motion mismatch is known as the recoil process, and is represented by a jagged line which provides information on the evolution of r_{1A} (r_{1b}). In other words on the coupling of reaction and transfer modes.

6.1   General derivation

6.1.1

We proceed now to derive the transition amplitude for the reaction (cf. Fig.)

$$A + a(= b + 1) \longrightarrow B(= A + 1) + b. \qquad (6.1.1)$$
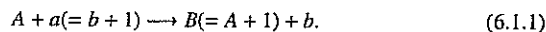
Let us/*now* assume that the nucleon bound initially to the core b is in a single–particle state with orbital and total angular momentum l_i and j_i respectively, and that the nucleon in the final state (bound to core A) is in the l_f, j_f state. The total spin and magnetic quantum numbers of nuclei A, a, B, b are $\{J_A, M_A\}, \{J_a, M_a\}, \{J_B, M_B\}, \{J_b, M_b\}$ respectively. Denoting ξ_A and ξ_b the intrinsic coordinates of the wavefunctions describing the structure of nuclei A and b respectively, and r_{An} and r_{bn} the relative coordinates of the transferred nucleon with respect to the CM of nuclei A and b respectively, one can

For a simplified version we refer to App. 6.E, while for an alternative derivation within the framework of knock-out reaction cf. App. 6.F.

write the "intrinsic" wavefunctions of the colliding nuclei A, a as

$$\phi_{M_A}^{J_A}(\xi_A),$$

$$\Psi(\xi_b, \mathbf{r}_{b1}) = \sum_{m_i} \langle J_b \ j_i \ M_b \ m_i | J_a \ M_a \rangle \phi_{M_b}^{J_b}(\xi_b) \psi_{m_i}^{j_i}(\mathbf{r}_{bn}, \sigma), \qquad (6.1.2)$$

while the "intrinsic" wavefunctions describing the structure of nuclei B and b are

$$\phi_{M_b}^{J_b}(\xi_b),$$

$$\Psi(\xi_A, \mathbf{r}_{A1}) = \sum_{m_f} \langle J_A \ j_f \ M_A \ m_f | J_B \ M_B \rangle \phi_{M_A}^{J_A}(\xi_A) \psi_{m_f}^{j_f}(\mathbf{r}_{An}, \sigma). \qquad (6.1.3)$$

For an unpolarized incident beam (sum over M_A, M_a and divide by $(2J_A + 1), (2J_a + 1)$) and assuming that one does not detect the final polarization (sum over M_B, M_b), the differential cross section in the DWBA can be written as

$$\frac{d\sigma}{d\Omega} = \frac{k_f}{k_i} \frac{\mu_i \mu_f}{4\pi^2 \hbar^4} \frac{1}{(2J_A + 1)(2J_a + 1)}$$

$$\times \sum_{\substack{M_A, M_a \\ M_B, M_b}} \left| \sum_{m_i, m_f} \langle J_b \ j_i \ M_b \ m_i | J_a \ M_a \rangle \langle J_A \ j_f \ M_A \ m_f | J_B \ M_B \rangle T_{m_i, m_f} \right|^2. \qquad (6.1.4)$$

The transition amplitude T_{m_i, m_f} is

$$T_{m_i, m_f} = \sum_{\sigma} \int d\mathbf{r}_f d\mathbf{r}_{bn} \chi^{(-)*}(\mathbf{r}_f) \psi_{m_f}^{j_f *}(\mathbf{r}_{An}, \sigma) V(\mathbf{r}_{bn}) \psi_{m_i}^{j_i}(\mathbf{r}_{bn}, \sigma) \chi^{(+)}(\mathbf{r}_i), \qquad (6.1.5)$$

where

$$\psi_{m_i}^{j_i}(\mathbf{r}_{An}, \sigma) = u_{j_i}(r_{bn}) \left[Y^{l_i}(\hat{r}_i) \chi(\sigma) \right]_{j_i m_i} \qquad (6.1.6)$$

is the single–particle wavefunction describing the motion of the nucleon to be transferred, in the initial state. Similarly for $\psi_{m_f}^{j_f}$. The incoming and outgoing distorted waves are

$$\chi^{(+)}(\mathbf{k}_i, \mathbf{r}_i) = \frac{4\pi}{k_i r_i} \sum_{l'} i^{l'} e^{i\sigma_{l'}} g_{l'}(\hat{r}_i) \left[Y^{l'}(\hat{r}_i) Y^{l'}(\hat{k}_i) \right]_0^0, \qquad (6.1.7)$$

and

$$\chi^{(-)*}(\mathbf{k}_f, \mathbf{r}_f) = \frac{4\pi}{k_f r_f} \sum_{l} i^{-l} e^{i\sigma_l} f_l(\hat{r}_f) \left[Y^{l}(\hat{r}_f) Y^{l}(\hat{k}_f) \right]_0^0, \qquad (6.1.8)$$

respectively. Now,

$$\left[Y^l(\hat{r}_f) Y^l(\hat{k}_f) \right]_0^0 \left[Y^{l'}(\hat{r}_i) Y^{l'}(\hat{k}_i) \right]_0^0 = \sum_K ((ll)_0 (l'l')_0 | (ll')_K (ll')_K)_0$$

$$\times \left\{ \left[Y^l(\hat{r}_f) Y^{l'}(\hat{r}_i) \right]^K \left[Y^l(\hat{k}_f) Y^{l'}(\hat{k}_i) \right]^K \right\}_0^0. \qquad (6.1.9)$$

The $9j$–symbol can be explicitly evaluated to give,

$$((ll)_0 (l'l')_0 | (ll')_K (ll')_K)_0 = \sqrt{\frac{2K+1}{(2l+1)(2l'+1)}}, \qquad (6.1.10)$$

while the coupled expression can be written as

~~and the angular momenta coupling is~~

$$\left\{\left[Y^l(\hat{r}_f)Y^{l'}(\hat{r}_i)\right]^K\left[Y^l(\hat{k}_f)Y^{l'}(\hat{k}_i)\right]^K\right\}_0^0 = \sum_M \langle K\,K\,M\,-M|0\,0\rangle\left[Y^l(\hat{r}_f)Y^{l'}(\hat{r}_i)\right]_M^K$$

$$\times\left[Y^l(\hat{k}_f)Y^{l'}(\hat{k}_i)\right]_{-M}^K = \sum_M \frac{(-1)^{K+M}}{\sqrt{2K+1}}\left[Y^l(\hat{r}_f)Y^{l'}(\hat{r}_i)\right]_M^K\left[Y^l(\hat{k}_f)Y^{l'}(\hat{k}_i)\right]_{-M}^K.$$

(6.1.11)

Thus,

$$\left[Y^l(\hat{r}_f)Y^l(\hat{k}_f)\right]_0^0\left[Y^{l'}(\hat{r}_i)Y^{l'}(\hat{k}_i)\right]_0^0 =$$

$$\sum_{K,M}\frac{(-1)^{K+M}}{\sqrt{(2l+1)(2l'+1)}}\left[Y^l(\hat{r}_f)Y^{l'}(\hat{r}_i)\right]_M^K\left[Y^l(\hat{k}_f)Y^{l'}(\hat{k}_i)\right]_{-M}^K. \quad (6.1.12)$$

For the angular integral to be different from zero, the integrand must be coupled to zero angular momentum (scalar). Noting that the only variables over which one integrates in the above expression are $\hat{r}_i, \hat{r}_f$, we have to couple the remaining functions of the angular variables, namely the wavefunctions $\psi_{m_f}^{j_f*}(\mathbf{r}_{An},\sigma) = (-1)^{j_f-m_f}\psi_{-m_f}^{j_f}(\mathbf{r}_{An},-\sigma)$ and $\psi_{m_i}^{j_i}(\mathbf{r}_{bn},\sigma)$ to angular momentum K, as well as to fulfill $M = m_f - m_i$. Let us then consider

$$(-1)^{j_f-m_f}\psi_{-m_f}^{j_f}(\mathbf{r}_{An},-\sigma)\psi_{m_i}^{j_i}(\mathbf{r}_{bn},\sigma) = (-1)^{j_f-m_f}u_{j_f}(r_{An})u_{j_i}(r_{bn})$$

$$\times\sum_P\langle j_f\,j_i\,-m_f\,m_i|P\,m_i-m_f\rangle\left\{\left[Y^{l_f}(\hat{r}_{An})\chi^{1/2}(-\sigma)\right]^{j_f}\left[Y^{l_i}(\hat{r}_{bn})\chi^{1/2}(\sigma)\right]^{j_i}\right\}_{m_i-m_f}^P.$$

(6.1.13)

?? Gregory

$\sigma = m_s = \pm\frac{1}{2}$

$\chi^{1/2}(-\sigma)$

Recoupling the spherical harmonics to angular momentum K and the spinors to $S = 0$, only one term survives the angular integral in (6.1.5) namely

$$(-1)^{j_f-m_f}u_{j_f}(r_{An})u_{j_i}(r_{bn})((l_f\tfrac{1}{2})_{j_f}(l_i\tfrac{1}{2})_{j_i}|(l_fl_i)_K(\tfrac{1}{2}\tfrac{1}{2})_0)_K$$

$$\times\langle j_f\,j_i\,-m_f\,m_i|K\,m_i-m_f\rangle\left[Y^{l_f}(\hat{r}_{An})Y^{l_i}(\hat{r}_{bn})\right]_{m_i-m_f}^K[\chi(-\sigma)\chi(\sigma)]_0^0. \quad (6.1.14)$$

Making use of the fact that the sum over spins yields a factor $-\sqrt{2}$, and in keeping with the fact that $M = m_f - m_i$, one obtains,

$$T_{m_i,m_f} = (-1)^{j_f-m_f}\frac{-16\sqrt{2}\pi^2}{k_fk_i}\sum_{ll'}i^{l'-l}e^{\sigma_f^l+\sigma_i^{l'}}\sum_K((l_f\tfrac{1}{2})_{j_f}(l_i\tfrac{1}{2})_{j_i}|(l_fl_i)_K(\tfrac{1}{2}\tfrac{1}{2})_0)_K$$

$$\times\langle j_f\,j_i\,-m_f\,m_i|K\,m_i-m_f\rangle\left[Y^l(\hat{k}_f)Y^{l'}(\hat{k}_i)\right]_{m_i-m_f}^K\int dr_fdr_{bn}\frac{f_l(r_f)g_{l'}(r_i)}{r_fr_i}$$

$$\times u_{j_f}(r_{An})u_{j_i}(r_{bn})V(r_{bn})(-1)^{K+m_f-m_i}\left[Y^l(\hat{r}_f)Y^{l'}(\hat{r}_i)\right]_{m_f-m_i}^K\left[Y^{l_f}(\hat{r}_{An})Y^{l_i}(\hat{r}_{bn})\right]_{m_i-m_f}^K.$$

(6.1.15)

Again, the only term of the expression

$$(-1)^{K+m_f-m_i}\left[Y^l(\hat{r}_f)Y^{l'}(\hat{r}_i)\right]_{m_f-m_i}^K\left[Y^{l_f}(\hat{r}_{An})Y^{l_i}(\hat{r}_{bn})\right]_{m_i-m_f}^K =$$

$$(-1)^{K+m_f-m_i}\sum_P\langle K\,K\,m_f-m_i\,m_i-m_f|P\,0\rangle\left\{\left[Y^l(\hat{r}_f)Y^{l'}(\hat{r}_i)\right]^K\left[Y^{l_f}(\hat{r}_{An})Y^{l_i}(\hat{r}_{bn})\right]^K\right\}_0^P$$

which survives after angular integration is the one with $P = 0$, that is,

$$\frac{1}{\sqrt{(2K+1)}} \left\{ \left[Y^l(\hat{r}_f) Y^{l'}(\hat{r}_i) \right]^K \left[Y^{l_f}(\hat{r}_{An}) Y^{l_i}(\hat{r}_{bn}) \right]^K \right\}_0^0 =$$

$$\frac{1}{\sqrt{(2K+1)}} \sum_{M_K} \langle K\ K\ M_K\ -M_K | 0\ 0 \rangle \left[Y^l(\hat{r}_f) Y^{l'}(\hat{r}_i) \right]^K_{M_K}$$

$$\times \left[Y^{l_f}(\hat{r}_{An}) Y^{l_i}(\hat{r}_{bn}) \right]^K_{-M_K} = \frac{1}{\sqrt{(2K+1)}} \sum_{M_K} \frac{(-1)^{K+M_K}}{\sqrt{(2K+1)}} \left[Y^l(\hat{r}_f) Y^{l'}(\hat{r}_i) \right]^K_{M_K}$$

$$\times \left[Y^{l_f}(\hat{r}_{An}) Y^{l_i}(\hat{r}_{bn}) \right]^K_{-M_K} =$$

$$\frac{1}{2K+1} \sum_{M_K} (-1)^{K+M_K} \left[Y^l(\hat{r}_f) Y^{l'}(\hat{r}_i) \right]^K_{M_K} \left[Y^{l_f}(\hat{r}_{An}) Y^{l_i}(\hat{r}_{bn}) \right]^K_{-M_K},$$

(6.1.2)

an expression which is spherically symmetric. One can evaluate it for a particular configuration, in particular setting $\hat{r}_f = \hat{z}$ and the center of mass A, b, n in the $x - z$ plane (see Fig. 6.1.1). Once the orientation in space of this "standard" configuration is specified (with, for example, a rotation $0 \le \alpha \le 2\pi$ around $\hat{z}$, a rotation $0 \le \beta \le \pi$ around the new x axis and a rotation $0 \le \gamma \le 2\pi$ around $\hat{r}_{bB}$), the only remaining angular coordinate is θ, while the integral over the other three angles yields a $8\pi^2$. Setting $\hat{r}_f = \hat{z}$ one obtains

through

$$\left[Y^l(\hat{r}_f) Y^{l'}(\hat{r}_i) \right]^K_{M_K} = \langle l\ l'\ 0\ M_K | K\ M_K \rangle \sqrt{\frac{2l+1}{4\pi}} Y^{l'}_{M_K}(\hat{r}_i). \qquad (6.1.16)$$

Because of $M = m_i - m_f$ and $m = m_f$, $T_{m_i, m_f} \equiv T_{m, M}$ where

$$T_{m,M} = (-1)^{j_f - m} \frac{-64\sqrt{2}\pi^{7/2}}{k_f k_i} \sum_{l l'} i^{l'-l} e^{\sigma'_l + \sigma_{l'}} \sqrt{2l+1} \sum_K \frac{(-1)^K}{2K+1} ((l_f \tfrac{1}{2})_{j_f} (l_i \tfrac{1}{2})_{j_i} | (l_f l_i)_K (\tfrac{1}{2}\tfrac{1}{2})_0)_K$$

$$\times \langle j_f\ j_i\ -m\ M+m | K\ M \rangle \left[Y^l(\hat{k}_f) Y^{l'}(\hat{k}_i) \right]^K_M \int dr_f dr_{bn} \frac{f_l(r_f) g_{l'}(r_i)}{r_f r_i}$$

$$\times u_{j_f}(r_{An}) u_{j_i}(r_{bn}) V(r_{bn}) \sum_{M_K} (-1)^{M_K} \langle l\ l'\ 0\ M_K | K\ M_K \rangle \left[Y^{l_f}(\hat{r}_{An}) Y^{l_i}(\hat{r}_{bn}) \right]^K_{-M_K} Y^{l'}_{M_K}(\hat{r}_i).$$

$$(6.1.17)$$

We now turn our attention to the sum

$$\sum_{\substack{M_A, M_a \\ M_B, M_b}} \left| \sum_{m, M} \langle J_b\ j_i\ M_b\ m_i | J_a\ M_a \rangle \langle J_A\ j_f\ M_A\ m_f | J_B\ M_B \rangle T_{m,M} \right|^2, \qquad (6.1.18)$$

found in the expression for the differential cross section (6.1.4). For any given value m', M' of m, M, the sum will be

appearing

$$\sum_{M_a, M_b} |\langle J_b\ j_i\ M_b\ m_i | J_a\ M_a \rangle|^2 \sum_{M_A, M_B} |\langle J_A\ j_f\ M_A\ m_f | J_B\ M_B \rangle|^2 |T_{m', M'}|^2 =$$

$$\frac{(2J_a + 1)(2J_B + 1)}{(2j_i + 1)(2j_f + 1)} \sum_{M_a, M_b} |\langle J_b\ J_a\ M_b\ -M_a | j_i\ m_i \rangle|^2$$

$$\times \sum_{M_A, M_B} |\langle J_A\ J_B\ M_A\ -M_B | j_f\ m_f \rangle|^2 |T_{m', M'}|^2, \qquad (6.1.19)$$

by virtue of the symmetry property of Clebsch–Gordan coefficients

$$\langle J_b\ j_i\ M_b\ m_i | J_a\ M_a \rangle = (-1)^{J_b - M_b} \sqrt{\frac{(2J_a + 1)}{(2j_i + 1)}} \langle J_b\ J_a\ M_b\ -M_a | j_i\ m_i \rangle. \qquad (6.1.20)$$

The sum over the Clebsch–Gordan coefficients in (6.1.19) is one, so (6.1.18) is just

$$\frac{(2J_a + 1)(2J_b + 1)}{(2j_i + 1)(2j_f + 1)} \sum_{m,M} |T_{m,M}|^2, \qquad (6.1.21)$$

and the differential cross section turns out to be

$$\frac{d\sigma}{d\Omega} = \frac{k_f}{k_i}\frac{\mu_i\mu_f}{4\pi^2\hbar^4}\frac{(2J_B + 1)}{(2j_i + 1)(2j_f + 1)(2J_A + 1)} \sum_{m,M} |T_{m,M}|^2. \qquad (6.1.22)$$

where

$$T_{m,M} = \sum_{KII'} (-1)^{-m} \langle j_f\ j_i\ -m\ M + m | K\ M \rangle \left[Y^l(\hat{k}_f) Y^{l'}(\hat{k}_i) \right]_M^K t_{ll'}^K. \qquad (6.1.23)$$

Orienting $\hat{k}_i$ along the incident z direction *leads to,*

$$\left[Y^l(\hat{k}_f) Y^{l'}(\hat{k}_i) \right]_M^K = \langle l\ l'\ M\ 0 | K\ M \rangle \sqrt{\frac{2l' + 1}{4\pi}} Y_M^l(\hat{k}_f), \qquad (6.1.24)$$

and

$$T_{m,M} = \sum_{KII'} (-1)^{-m} \langle l\ l'\ M\ 0 | K\ M \rangle \langle j_f\ j_i\ -m\ M + m | K\ M \rangle Y_M^l(\hat{k}_f) t_{ll'}^K, \qquad (6.1.25)$$

with

$$t_{ll'}^K = (-1)^{K + j_f}\frac{-32\sqrt{2}\pi^3}{k_f k_i}i^{l' - l}e^{\sigma_f^l + \sigma_i^{l'}}\frac{\sqrt{(2l + 1)(2l' + 1)}}{2K + 1}((l_f\tfrac{1}{2})_{j_f}(l_i\tfrac{1}{2})_{j_i}|(l_f l_i)_K(\tfrac{1}{2}\tfrac{1}{2})_0)_K$$

$$\times \int dr_f\ dr_{bn} d\theta r_{bn}^2 \sin\theta\ r_f\frac{f_l(r_f)g_{l'}(r_i)}{r_i}u_{j_f}(r_{An})u_{j_i}(r_{bn})V(r_{bn})$$

$$\times \sum_{M_K}(-1)^{M_K}\langle l\ l'\ 0\ M_K | K\ M_K \rangle \left[Y^{l_f}(\hat{r}_{An})Y^{l_i}(\hat{r}_{bn}) \right]_{-M_K}^K Y_{M_K}^{l'}(\hat{r}_i). \qquad (6.1.26)$$

6.1.1   Coordinates

6.1.2

To perform the integral in (6.1.26), one needs the expression of $r_i, r_{An}, \hat{r}_{An}, \hat{r}_{bn}, \hat{r}_i$ in term of the integration variables r_f, r_{bn}, θ. Because one is interested in evaluating these quantities in the particular configuration depicted in Fig. 6.1.2, one has

$$\mathbf{r}_f = r_f\hat{z}, \qquad (6.1.27)$$

$$\mathbf{r}_{bn} = -r_{bn}(\sin\theta\hat{x} + \cos\theta\hat{z}), \qquad (6.1.28)$$

$$\mathbf{r}_{Bn} = \mathbf{r}_f + \mathbf{r}_{bn} = -r_{bn}\sin\theta\hat{x} + (r_f - r_{bn}\cos\theta)\hat{z}. \qquad (6.1.29)$$
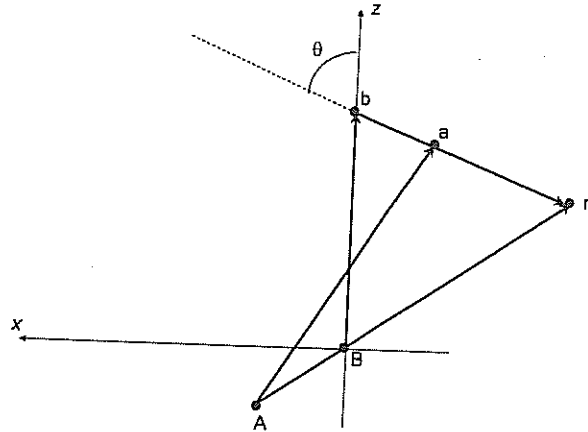
Figure 6.1.2: Coordinate system in the "standard" configuration. Note that $\mathbf{r}_f \equiv \mathbf{r}_{Bb}$, and $\mathbf{r}_i \equiv \mathbf{r}_{Aa}$.

One can then write

$$\mathbf{r}_{An} = \frac{A+1}{A}\mathbf{r}_{Bn} = -\frac{A+1}{A}r_{bn}\sin\theta\,\hat{x} + \frac{A+1}{A}(r_f - r_{bn}\cos\theta)\,\hat{z}, \qquad (6.1.30)$$

$$\mathbf{r}_{an} = \frac{b}{b+1}\mathbf{r}_{bn} = -\frac{b}{b+1}r_{bn}(\sin\theta\,\hat{x} + \cos\theta\,\hat{z}), \qquad (6.1.31)$$

and

$$\mathbf{r}_i = \mathbf{r}_{An} - \mathbf{r}_{an} = -\frac{2A+1}{(A+1)A}r_{bn}\sin\theta\,\hat{x} + \left(\frac{A+1}{A}r_f - \frac{2A+1}{(A+1)A}r_{bn}\cos\theta\right)\hat{z}, \quad (6.1.32)$$

where A, b are the number of nucleons of nuclei A and b respectively.

6.1.2 Zero range approximation

In the zero range approximation,

$$\int dr_{bn}r_{bn}^2 u_{ji}(r_{bn})V(r_{bn}) = D_0; \quad u_{ji}(r_{bn})V(r_{bn}) = \delta(r_{bn})/r_{bn}^2. \qquad (6.1.33)$$

It can be shown (see Fig. 6.1.2) that for $r_{bn} = 0$

$$\mathbf{r}_{An} = \frac{m_A+1}{m_A}\mathbf{r}_f$$

$$\mathbf{r}_i = \frac{m_A+1}{m_A}\mathbf{r}_f. \qquad (6.1.34)$$

$$\mathbf{r}_{An} = \frac{m_A+1}{m_A}\vec{r}_f \quad , \quad \mathbf{r}_i = \frac{m_A+1}{m_A}\vec{r}_f . \quad (6.1.34)$$

One then obtains

$$t^K_{ll'} = \frac{-16\sqrt{2}\pi^2}{k_f k_i}(-1)^K \frac{D_0}{\alpha} i^{l'-l} e^{\sigma'_f + \sigma'_i} \frac{\sqrt{(2l+1)(2l'+1)(2l_i+1)(2l_f+1)}}{2K+1} ((l_f\tfrac{1}{2})_{j_f}(l_i\tfrac{1}{2})_{j_i}|(l_f l_i)_K(\tfrac{1}{2}\tfrac{1}{2})_0)_K$$

$$\times \langle l\, l'\, 0\, 0|K\, 0\rangle\langle l_f\, l_i\, 0\, 0|K\, 0\rangle \int dr_f\, f_i(r_f) g_{l'}(\alpha r_f) u_{j_f}(\alpha r_f),$$

(6.1.35)

with

$$\alpha = \frac{A+1}{A}.$$

(6.1.36)

6.2 Examples and Applications

In this section we discuss some examples which illustrate the workings of single–particle transfer processes at large, and in particular the flavour of the limitations by which nuclear structure studies suffer, when this specific probe to study quasiparticle properties is not operative. Let us in fact start with such an example.

6.2.1 Dressing of single–particle states: parity inversion in ^{11}Li

[handwritten insertion above title: two-neutron]

The $N = 6$ isotope of $^{9}_{3}$Li displays quite ordinary structural properties and can, at first glance, be thought of a ~~two-neutron~~ hole system in the $N = 8$ closed shell. That this is not the case emerges clearly from the fact that ^{10}Li is not bound, the lowest virtual $(1/2^+)$ and resonant $(1/2^-)$ states testify to the fact that, in the present case, the $N = 6$ is a far better magic neutron number than $N = 8$. Furthermore, that the unbound $s_{1/2}$ state lies lower than the unbound $p_{1/2}$ state, in plain contradiction with static mean field theory. Dressing the (standard) mean field single particle states with vibrations, mostly with the core quadrupole vibration, through polarization (effective masslike) and correlation diagrams (vacuum zero point fluctuations (ZPF)) diagrams, similar to those associated with the (lowest order) Lamb shift Feynman diagrams, move the $s_{1/2}$ and $p_{1/2}$ mean field levels around. In particular the $p_{1/2}$ from a bound state (≈ -1.2MeV) to a resonant state lying at ≈ 0.5 MeV (Pauli principle, vacuum ZPF process) *6.B.1*

How can one check that CO and PO like processes as the ones shown in Fig. and (cf. also Fig.) are the basic processes dressing the odd neutron of ^{10}Li, and thus the mechanism at the basis of parity inversion? The answer is, forcing these virtual processes to become real. While this is not easy to accomplish in one–particle transfer processes involving the unbound $s_{1/2}$ and $p_{1/2}$, ^{10}Li virtual and resonant states, it can done with the help of two–particle transfer processes, namely that associated with inverse kinematics (p,t) reaction ^{3}H(^{11}Li,^{9}Li(2.69MeV; $1/2^-$))^{3}H (cf. Fig. and Chs.). Such a reaction is feasible, in keeping with the fact that, adding a neutron to ^{10}Li leads to a bound state (see Fig.). In fact, $^{11}_{3}$Li displays a two–neutron separation energy $S_{2n} \approx 400$ keV (for further details we refer to Ch. , Sect.). The price to pay for not being able to use the specific probe for single–particle modes (one–particle transfer), is that of adding to the self–energy contributions in question those corresponding to vertex corrections (for details cf. Sect. (application 2n–transfer)). Within the present context, it is difficult if not impossible to talk about single–particle motion without also referring to collective vibrational states

[handwritten marginal annotations, left side:]
and has been studied (Tanihata et al, 2008)
be
A
7 and 8 (two–nucleon transfer; 7 for–malism, 8; applications and examples)

[handwritten marginal annotations, right side:]
cf. App. C
6.1.3 (I)
respectively
6.1.4
6.1.3 (II)
6.1.1
8
App. 6D, Figs. 6.D.1 and 6.D.2 and Ch. 8
8.2

$$|0^+\rangle = \sqrt{0.40}\,|s_{1/2}^2(0)\rangle$$
$$+\sqrt{0.58}\,|p_{1/2}^2(0)\rangle$$
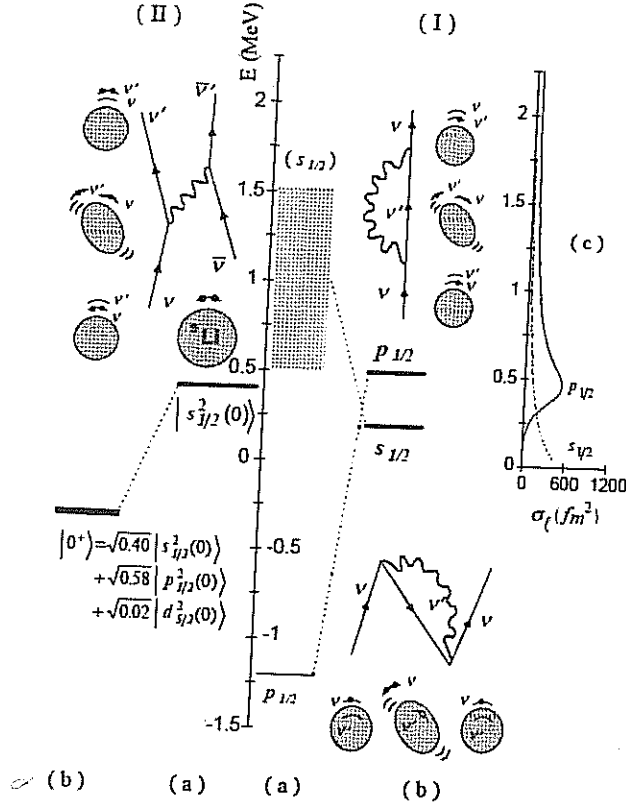$$+\sqrt{0.02}\,|d_{5/2}^2(0)\rangle$$

Figure 6.1.3: (I) Single-particle neutron resonances in ^{10}Li. In (a) the position of the levels $s_{1/2}$ and $p_{1/2}$ calculated making use of mean-field theory is shown (hatched area and thin horizontal line, respectively). The coupling of a single-neutron (upward pointing arrowed line) to a vibration (wavy line) calculated making use of the Feynman diagrams displayed in (b) (schematically depicted also in terms of either solid dots (neutron) or open circles (neutron hole) moving in a single-particle level around or in the ^{9}Li core (hatched area)), leads to conspicuous shifts in the energy centroid of the $s_{1/2}$ and $p_{1/2}$ resonances (shown by thick horizontal lines) and eventually to an inversion in their sequence. In (c) we show the calculated partial cross-section 1 for neutron elastic scattering off ^{9}Li. (II) The two-neutron system ^{11}Li. We show in (a) the meanfield picture of ^{11}Li, where two neutrons (solid dots) move in time-reversal states around the core ^{9}Li (hatched area) in the $s_{1/2}$ resonance leading to an unbound $s_{1/2}^2(0)$ state where the two neutrons are coupled to zero angular momentum. The exchange of vibrations between the two neutrons shown in the upper part of the figure leads to a density-dependent interaction which, added to the nucleon-nucleon interaction, correlates the two-neutron system leading to a bound state $|0^+\rangle$, where the two neutrons move with probability 0.40, 0.58 and 0.02 in the two-particle configurations $s_{1/2}^2(0)$, $p_{1/2}^2(0)$ and $d_{5/2}^2(0)$, respectively.
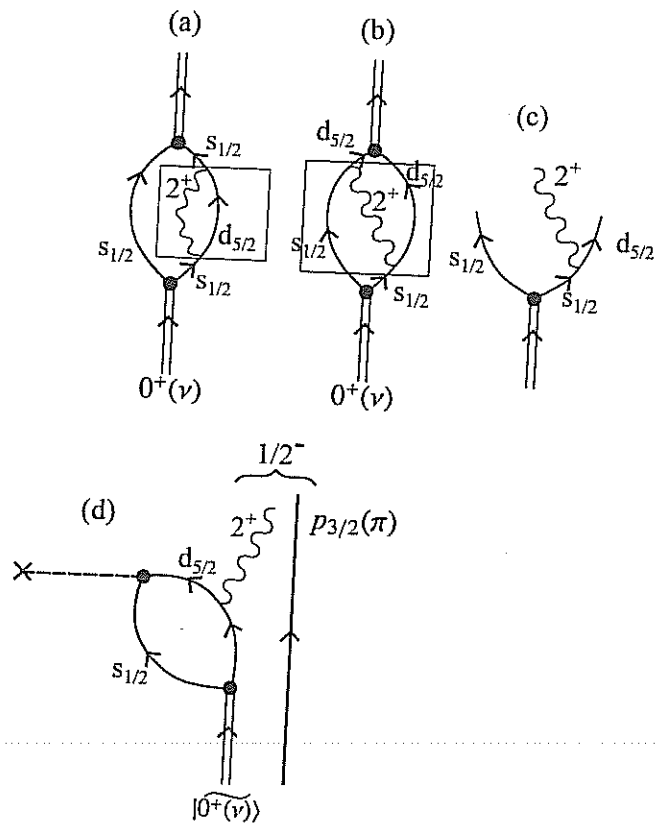
Figure 6.1.4: (a)Self–energy (see boxed process) and (b) vertex (pairing induced interaction boxed process) renormalization process, both associate with (c) a (two–particle)–(quadrupole vibration) intermediate (virtual state) which can be forced to became real in a (p,t) reaction ^{1}H(^{11}Li,^{9}Li)^{3}H exciting the first excited state (2.69MeV;1/2$^-$) of ^{9}Li (see Ch.   .)

8 (examples and applications
        two-nucleon transfer)

6.1.3 (II)

in connection of both structure and reaction processes. Si-

6.A. MINIMAL REQUIREMENTS FOR A CONSISTENT MEAN FIELD THEORY11 *milarly,*

6.1.4 (a) and (b)

6

5

(cf. e.g. Fig. ~~)~~ ~~both in structure and reactions as well~~ as to talk about pair addition and pair substraction correlations, without at the same time talking about vibrations *concerning both* ~~and dressed quasiparticle~~ motion (see e.g. Figs. ~~), And this~~ again ~~structure and~~ ~~reactions.~~ Within the framework of the present monograph, the above facts imply that Chapters ~~ (inelastic), ~~ (one-particle transfer) ~~and ~~ and ~~ (two-particle transfer and applications) form a higher unity. ~~The unity extending~~ also to ~~Ch ~~ (knock-out

excited

reactions), if one also considers the question of final state interactions, and thus of the *the content* possibility that the population of the state $1/2^-$ depicted in Fig. ~~ receives contri- *of App. F* butions other, and more involved, than those associated with the direct two-nucleon 6.1.4 (d) pick-up depicted (for details cf. Ch. ~~ 8; cf. also

Potel et al (2010)]. This unity extends

Appendix 6.A   Minimal requirements for a consistent mean field theory

In what follows th question of why, rigorously speaking, one cannot talk about single-particle motion, let alone spectroscopic factor, not even within the framework of Hartree-Fock theory, is briefly touched upon.   6.A.1

As can be seen from Fig. ~~ the minimum requirements of selfconsistency to be imposed upon single particle motion requires both non-locality in space (HF) and in time (TDHF)

$$i\hbar \frac{\partial \rho_\nu}{\partial t} = -\frac{\hbar^2}{2m}\nabla^2 \varphi_\nu(x,t) + \int dx' dt' U(x-x', t-t')\varphi_\nu(x',t') \quad (6.A.1)$$

)

and consequently also of collective vibrations and, consequently, from their inter-weaving to dressed single-particles (quasiparticles), let alone renormalized collective *(Brink and Broglia,* modes. Assuming for simplicity infinite nuclear matter (confined by a constant poten- *2005)* tial of depth V_0), and thus plane wave solutions, the above time-dependent Schrödinger equation leads to the quasiparticle dispersion relation (cf. e.g. ~~)

$$\hbar\omega = \frac{\hbar^2 k^2}{2m^*} + \frac{m}{m^*}V_0, \quad (6.A.2)$$

where the effective mass

$$m^* = \frac{m_k m_\omega}{m}, \quad (6.A.3)$$

in the product of the k-mass

$$m_k = m\left(1 + \frac{m}{\hbar^2 k}\frac{\partial U}{\partial k}\right)^{-1} \quad (6.A.4)$$

closely connected with the Pauli principle $\left(\frac{\partial U}{\partial k} \approx \frac{\partial U_z}{\partial k}\right)$, while the ω-mass   (6.A.2)

$$m_\omega = m\left(1 - \frac{\partial U}{\partial \hbar\omega}\right) \quad (6.A.5)$$
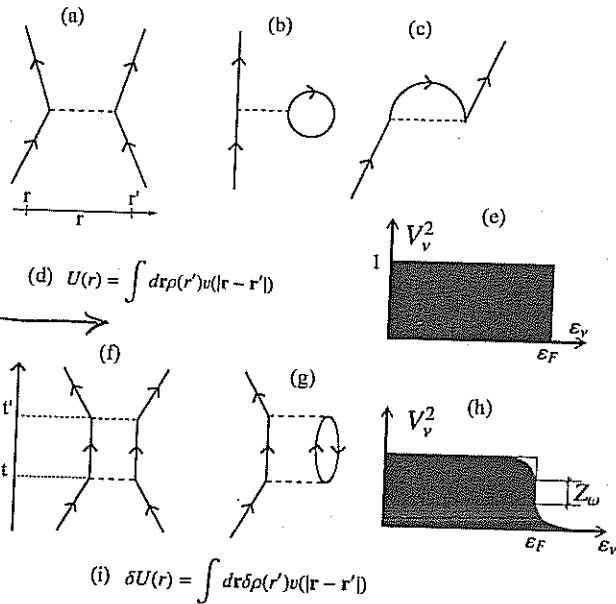
results from the dressing of the nucleon through the coupling with the (quasi) bosons. Because typically $m_k \approx 0.7m$ and $m_\omega \approx 1.4m$ $m^* \approx m$, one could be tempted to conclude that the results embodied in the dispersion relation ~~ reflects that the distri-bution of levels around the Fermi energy can be described in terms of the solutions of

$$(d') \quad U_x(r, r') = -\sum_{i} \varphi_i^*(\vec{r}\,') \, v(|\vec{r} - \vec{r}\,'|) \, \varphi_i(\vec{r})$$
$$(\varepsilon_i \le \varepsilon_F)$$

(a) (b) (c)

(d) $U(r) = \int dr \rho(r') v(|r - r'|)$

(e) V_ν^2 ε_ν ε_F

(f) (g)

(h) V_ν^2 Z_ω ε_F ε_ν

(i) $\delta U(r) = \int dr \delta \rho(r') v(|r - r'|)$

(non - local (d'))

Figure 6.A.1: (a)Scattering of two nucleons through the bare NN interaction $v|r - r'|$, (b) contribution to the direct (U, Hartree) and (c) to the exchange (U_x, Fock) potential, resulting in (d) the (static) selfconsistent relation between potential and density, which (e) uncouples occupied ($\varepsilon_\nu \le \varepsilon_F$) from empty states ($\varepsilon_\nu > \varepsilon_F$), (f) multiple scattering of two nucleons lead, through processes like the one depicted in (g), eventually propagated to all orders, to: (h) softening of the discontinuity of the occupancy of levels at ε_F, as well as to: (i) generalization of the static selfconsistency into a dynamic relation encompassing also collective vibrations (Time–dependent HF solutions of the nuclear Hamiltonian, conserving energy weighted...).
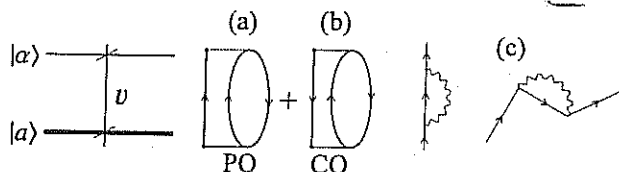
sum rules (EWSR)

Figure 6.B.1: Two state schematic model describing the breaking of the strength of the pure single–particle state $|a\rangle$, through the coupling to collective vibrations (wavy line) associated with polarization (PO) and correlation (CO) processes.

6.A.1 (h)

a Schrödinger equation in which nucleons of mass equal to the bare nucleon mass m move in a Saxon–Woods potential of depth V_0.

Now, it can be shown that the occupancy of levels around ε_F is given by Z_ω (cf. Fig.) a quantity which is equal to $m/m_\omega \approx 0.7$. This, in keeping with the fact that the time the nucleon is coupled to the vibrations it cannot behave as a single–particle and can thus not contribute to e.g. the single–particle pickup cross section.

It is of notice that the selfconsistence requirements for the iterative solution of the Kohn–Sham equations

$$H^{KS}\varphi_\gamma(\mathbf{r}) = \lambda_\gamma\varphi_\gamma(\mathbf{r}),\qquad(6.A.6)$$

where

$$H^{KS} = -\frac{\hbar^2}{2m_e}\nabla^2 + U_H(\mathbf{r}) + V_{ext}(\mathbf{r}) + U_{xc}(\mathbf{r}),\quad\boxed{d}\qquad(6.A.7)$$

H^{KS} being known as the Kohn–Sham Hamiltonian, $V_{ext}(\mathbf{r})$ being the field created by the ions and acting on the electrons. Both the Hartree and the exchange–correlation potentials $U_H(\mathbf{r})$ and $U_{xc}(\mathbf{r})$ depend on the (local) density, hence on the whole set of wavefunctions $\varphi_\gamma(\mathbf{r})$. Thus, the set of KS–equations must be solve selfconsistently. (cf. e.g. Broglia et al. (2004) and refs. therein)

Appendix 6.B Model for single–particle strength function: Dyson equation

6.B.1

(App. 6.A)

In the previous section we introduce d the argument of the impossibility difficulty of defining a "bona fide" single–particle spectroscopic factor. It was done with the help of Feynman (NFT) diagrams. In what follows we essentially repeat the arguments, but this time in terms of Dyson's (Schwinger) language. For simplicity, we consider a two–level model where the pure single–particle state $|a\rangle$ couples to a more complicated state $|\alpha\rangle$, made out of a fermion (particle or hole), couple to a particle–hole excitation which, if iterated to all orders can give rise to a collective state (cf. Fig.). The Hamiltonian describing the system is

$$H = H_0 + U\qquad(6.B.1)$$

where

$$H_0|a\rangle = E_a|a\rangle,\qquad(6.B.2)$$

and

$$H_0|\alpha\rangle = E_\alpha|\alpha\rangle.\qquad(6.B.3)$$

Let us call $\langle a|U|\alpha\rangle = U_{a\alpha}$ and assume $\langle a|U|a\rangle = \langle\alpha|U|\alpha\rangle = 0$.

low case U

of Eq. (6.A.1) (see Fig. 6.A.1 (d) and (d')), remind very much those associated with the solution

associated

Making use of the solution of the Dyson equation (6.B.7), and of the relations (6.B.5) and (6.B.6), one can calculate the renormalized state $|\tilde{a}\rangle$ to be employed in working out the modified, single-particle transfer form factor.

CHAPTER 6. ONE-PARTICLE TRANSFER

From the secular equation ~~associated with H, namely~~

$$\begin{pmatrix} E_\alpha & U_{a\alpha} \\ U_{a\alpha} & E_a - E_i \end{pmatrix}\begin{pmatrix} C_\alpha(i) \\ C_a(i) \end{pmatrix} = 0,$$ (6.B.4)

and associated normalization condition

$$C_a^2(i) + C_\alpha^2(i) = 0,$$ (6.B.5)

one obtains

$$C_a^2(i) = \left(1 + \frac{U_{a\alpha}^2}{(E_\alpha - E_i)^2}\right)^{-1},$$ (6.B.6)

and

The energy of

$$\Delta E_a(E) = E_a - E = \frac{U_{a\alpha}^2}{E_a - E}.$$ (6.B.7)

~~The relations 6.B.6 and 6.B.7 allow one to write~~ the correlated state

$$|\tilde{a}\rangle = C_a(i)|a\rangle + C_\alpha(i)|\alpha\rangle,$$ 6.B.1   (6.B.8)

is obtained

~~the corresponding energy being provided~~ by the (iterative) solution of the Dyson equation 6.B.7, which propagate the bubble diagrams shown in Figs $\mathcal{R}$ (a) and (b) to infinite order leading to collective vibrations (see Fig. $\mathcal{R}$)   6.B.1 (c)

With the help of the definition $\mathcal{R}$, and making use of the fact that in the present case, $U \equiv \Delta E_a(E)$, one obtains

given in Eq. (6.A.5)

$$Z_\omega = C_a^2(i) = \left(\frac{m_\omega}{m}\right)^{-1}.$$ (6.B.9)

~~the solution of 6.B.7 together with the relations ?? and ?? lead to the quasiparticle state ?? to be employed in the calculation of the one-particle transfer transition amplitudes (cf. e.g. ?? and ??)~~

Appendix 6.C   The Lamb Shift

6.C.1

In Fig. $\mathcal{R}$ we display a schematic summary of the electron–photon processes, associated with Pauli principle corrections, leading to the splitting of the lowest s, p states of the hydrogen atom known as the Lamb shift.

In the upper part of the figure the predicted position of the electronic single–particle levels of the hydrogen atom as resulting from the solution of the Scrödinger equation (Coulomb field). In the lowest part of the figure one displays the electron of an hydrogen atom (upwards going arrowed line) in presence of vacuum ZPF (electron–positron pair plus photon, oyster–like diagram). Because the associate electron virtually occupies states already occupied by the hydrogen's electron, thus violating Pauli principle, one has to antisymmetrize the corresponding two–electron state. Such process gives rise to the exchange of the corresponding fermionic lines and thus to CO–like digrams as well as, through time ordering, to PO–like diagrams. The results provide a quantitative account of the experimental findings.
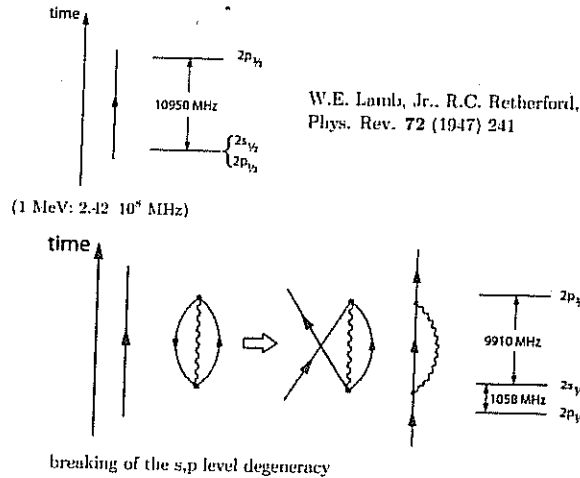
W.E. Lamb, Jr.. R.C. Retherford,
Phys. Rev. 72 (1947) 241

(1 MeV: 2.42 10⁸ MHz)

breaking of the s,p level degeneracy

Figure 6.C.1: Schematic representation of the processes associated with the Lamb shift.

Appendix 6.D Self–energy and vertex corrections

In Fig. *an example of the fact that in field theories (e.g. QED or NPT), nothing is really free and that e.g., the bare masss of a fermion (electron or nucleon), is the parameter one adjusts (m_R) so that the result of a measurement (cf. Fig.) gives the observed mass (single particle energy). In Fig. , lowest order diagrams associated with the renormalization of the fermion–boson interaction (vertex corrections) are given. The sum of contributions (a) and (b) can, in principle, be represented by a renormalized vertex (cf. digram (c)). It is of notice, however, that there is, as a rule, conspicuous interference (e.g. cancellation) in the nuclear case between vertex and self–energy contributions (cf. diagrams (a) and (b) of Fig.) a phenomenon closely related with conservation laws (generalized Ward identities)). In particular, cancellation in the case in which the bosonic modes are isoscalar. Consequently, one has to sum explicitly the different amplitudes with the corresponding phases and eventually take the modulus squared of the result to eventually obtain the quantities to be compared with the data, a fact that precludes the use of an effective (renormalized) vertex (cf. Fig.).

Within the framework of QED the above mentioned cancellations are exact implying that the interaction between one and two photon states vanishes (Furry theorem). The physics at the basis of the cancellation found in the nuclear case can be exemplified by looking at a spherical nucleus displaying a low–lying collective quadrupole zero–point vibration. The associated zero point fluctuations (ZPF) lead to time–dependent shapes with varied instantaneous values of the quadrupole moment, and of its orientation (dynamical spontaneous breaking of rotational invariance). In other words, a component of the ground state wavefunction ($|(j_p \otimes j_h^{-1})_{2^+} \otimes 2^+; 0^+)$) can be viewed as a gas of quadrupole (quasi) bosons, promoting a nucleon across the Fermi energy (particle–hole excitation) will lead to fermionic states which behave as having a positive (particle) and a negative (hole) effective quadrupole moment, in keeping with the fact that the closed shell system is spherical, thus carrying zero quadrupole moment.

(handwritten annotations in margins:)
6.D.2
6.D.1
really
m_R
a
(d) + (e)
and
6.D.2 ,
. C
ω – indepent
which
P

From here, the sign of the coupling vertices shown in the diagrams of Fig. 6.D.2.

the

Self-Energy (effective mass) processes
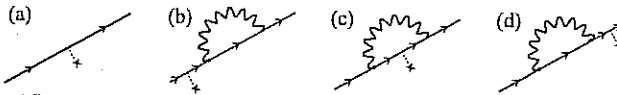
(a)   (b)   (c)   (d)

Figure 6.D.1: The result of the probing with an external field (dotted line started with a , 1975)
cross) of the properties (mass, single–particle energy, etc) of a fermion (e.g. an electron
or a nucleon, arrowed line) dressed through the coupling of (quasi) bosons (photons or
collective vibrations, wavy line), corresponds to the modulus squared of the sum of the
amplitudes associated with each of the four diagrams (a)–(d) (cf. Feynman, Theory of
fundamental processes).

Self-energy (effective-mass-like) processes,

and of the corresponding time-ordering processes

Vertex corrections

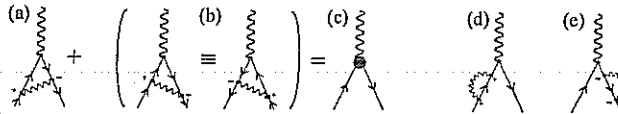(a)   (b)   (c)   (d)   (e)

Figure 6.D.2: These are triple–interaction vertex diagrams in which none of the incom-
ing lines can be detached from either of the other two by cutting one line. Migdal's
(1958) theorem states that, for phonons and electrons (Bardeen–Pines–Frölich mecha-
nism to break gauge invariance), vertex corrections can be neglected, but usually they   (1984)
are not negligible, in any case not in nuclei (cancellation) (cf. e.g. Anderson,)
sic notions of condensed matter physics). The solid circle in (c) represents the effective,
renormalized vertex.

Vertex corrections.

Appendix 6.E Single–nucleon transfer for pedestrians

In this Appendix we discuss some aspects of the relation existing between nuclear struc-
ture and one–particle transfer cross sections. To do so, we repeat some of the steps car-
ried out in the text but this time in the most simple and straightforward way, ignoring
the complications associated with the spin carried out by the particles, the spin–orbit
dependence of the optical model potential, the recoil effect, etc. We consider the case
of $A(d,p)A+1$ reaction, namely of neutron stripping. The intrinsic wave functions ψ_α
and ψ_β, where $\alpha = (A, d)$ and $\beta = ((A+1), p)$,

$$\psi_\alpha = \psi^{I_A}_{M_A}(\xi_A)\phi_d(\vec{r}_{np}), \tag{6.E.1a}$$

$$\psi_\beta = \psi^{I_{A+1}}_{M_{A+1}}(\xi_{A+1})$$
$$= \sum_{l,I'_A}(I'_A; l|I_{A+1})[\psi^{I'_A}_A(\xi_A)\phi^l(\vec{r}_n)]^{I_{A+1}}_{M_{A+1}-M_A}, \tag{6.E.1b}$$

where $(I'_A; l|I_{A+1})$ is a generalized fractional parentage coefficient. It is of notice that
this fractional parentage expansion is not well defined. In fact, as a rule,
$(I'_A; l|I_{A+1})\phi^l(\vec{r}_n)_{M_{A+1}-M_A}$ is an involved, dressed quasiparticle state containing only a
fraction of the "pure" single particle strength (cf. 'B'). For simplicity we assume the
expansion is operative. To further simplify the derivation, we assume we are dealing
with spinless particles. The variable $\vec{r}_{np}$ is the relative coordinate of the proton and the
neutron (see Fig.).

The transition matrix element can now be written as

$$T_{d,p} = \langle\psi^{I_{A+1}}_{M_{A+1}}(\xi_{A+1})\chi^{(-)}_p(k_p, \vec{r}_p), V'_\beta\psi^{I_A}_{M_A}(\xi_A)\chi^{(+)}_d(k_d, \vec{r}_d)\rangle$$

$$= \sum_{\substack{l,I'_A \\ M'_A}}(I'_A; l|I_{A+1})(I'_A M'_A l M_{A+1} - M'_A|I_{A+1} M_{A+1})$$

$$\times \int d\vec{r}_n d\vec{r}_p\chi^{*(-)}_p(k_p, \vec{r}_p)\phi^{*l}_{M_{A+1}-M'_A}(\vec{r}_n)(\psi^{I_A}_{M_A}(\xi_A), V'_\beta\psi^{I'_A}_{M'_A}(\xi_A))$$

$$\times \phi_d(\vec{r}_{np})\chi^{(+)}_d(k_d, \vec{r}_d)\,\delta_{I'_A,I_A}\,\delta_{M'_A,M_A}. \tag{6.E.2}$$

In the stripping approximation

$$V'_\beta = V_\beta(\xi, \vec{r}_\beta) - \bar{U}_\beta(r_\beta)$$
$$= V_\beta(\xi_A, \vec{r}_{pA}) + V_\beta(\vec{r}_{pn}) - \bar{U}_\beta(r_{pA}) \tag{6.E.3}$$

Then

$$(\psi^{I_A}_{M_A}(\xi_A), V'_\beta\psi^{I_A}_{M_A}(\xi_A)) = (\psi^{I_A}_{M_A}(\xi_A), V_\beta(\xi_A, \vec{r}_{pA})\psi^{I_A}_{M_A}(\xi_A))$$
$$+ (\psi^{I_A}_{M_A}(\xi_A), V_\beta(\vec{r}_{pn})\psi^{I_A}_{M_A}(\xi_A)) - \bar{U}_\beta(r_{pA}). \tag{6.E.4}$$

We assume

$$U_\beta(r_{pA}) = (\psi^{I_A}_{M_A}(\xi_A), V_\beta(\xi_A, \vec{r}_{pA})\psi^{I_A}_{M_A}(\xi_A)). \tag{6.E.5}$$

Then

$$(\psi^{I_A}_{M_A}(\xi_A), V'_\beta\psi^{I_A}_{M_A}(\xi_A)) = V_{np}(\vec{r}_{pn}) \tag{6.E.6}$$

Inserting eq. (6.E.6) into eq. (6.E.2) we obtain

$$T_{d,p} = \sum_l(I_A; l|I_{A+1})(I_A M_A l M_{A+1} - M_A|I_{A+1} M_{A+1})$$

$$\times \int d\vec{r}_n d\vec{r}_p\chi^{*(-)}_p(k_p, \vec{r}_p)\phi^{*l}_{M_{A+1}-M_A}(\vec{r}_n)V(\vec{r}_{pn})\phi_d(\vec{r}_{np})\chi^{(+)}_d(k_d, \vec{r}_d) \tag{6.E.7}$$